A comprehensive data-driven analysis framework for detecting impairments in brain function networks with resting state fMRI in HIV-infected individuals on cART

Sheeba Arnold Anteraper[4] · Kaundinya Gopinath[1] · Michael J. Hoch[1] · Drenna Waldrop-Valverde[2] · Donald Franklin[3] · Scott L. Letendre[3] · Susan Whitfield-Gabrieli[4] · Albert M. Anderson[1]

Abstract

Central nervous system (CNS) sequelae continue to be common in HIV-infected individuals despite combination antiretroviral therapy (cART). These sequelae include HIV-associated neurocognitive disorder (HAND) and virologic persistence in the CNS. Resting state functional magnetic resonance imaging (rsfMRI) is a widely used tool to examine the integrity of brain function and pathology. In this study, we examined 16 HIV-positive (HIV+) subjects and 12 age, sex, and race matched HIV seronegative controls (HIV−) whole-brain high-resolution rsfMRI along with a battery of neurocognitive tests. A comprehensive data-driven analysis of rsfMRI revealed impaired functional connectivity, with very large effect sizes in executive function, language, and multisensory processing networks in HIV+ subjects. These results indicate the potential of high-resolution rsfMRI in combination with advanced data analysis techniques to yield biomarkers of neural impairment in HIV.

Keywords HIV · resting state fMRI · high-resolution · functional connectivity · multi-voxel pattern analysis · MVPA · brain function networks · cognition · executive function · executive function · language · multi-sensory perception

Introduction

While HIV infection has become a treatable condition in the combination antiretroviral therapy (cART) era, it is clear that the infection has persistent, detrimental effects on the central nervous system (CNS). Among individuals on cART, cerebrospinal fluid (CSF) studies have shown elevated markers of inflammation, while neuroimaging studies have demonstrated increases in CNS membrane turnover and glial proliferation (Anderson et al. 2017; Harezlak et al. 2011). HIV-associated neurocognitive disorder (HAND)

Sheeba Arnold Anteraper and Kaundinya Gopinath are co-first authors, who made equal contributions to the paper

✉ Albert M. Anderson
   aande2@emory.edu

1   Emory University School of Medicine, Atlanta, GA, USA

2   Emory University School of Nursing, Atlanta, GA, USA

3   University of California At San Diego School of Medicine, La Jolla, San Diego, CA, USA

4   Northeastern University, Boston, MA, USA

remains highly prevalent (around 50%) in the era of cART (Abidin et al. 2020; Heaton et al. 2010) and is associated with diminished quality of life as well as an increase in mortality risk (Tozzi et al. 2003; Vivithanaporn et al. 2010). Additionally, building evidence demonstrates that the CNS is a reservoir of HIV persistence and thus a barrier to HIV cure (Lamers et al. 2016). A more comprehensive understanding of the effects of HIV on the CNS is therefore needed to most effectively address residual CNS impairment during cART.

About 70% of individuals suffering from HAND (Grant et al. 2014; Heaton et al. 2010) only exhibit asymptomatic neurocognitive impairment (ANI). HIV-infected individuals with ANI are at greater risk to deteriorate to severe neurocognitive impairment with time (Grant et al. 2014). Hence, it is critical to diagnose ANI at early stages so that targeted treatment could be administered when necessary. Unfortunately, standard neuropsychological (NP) tests are often not sufficiently sensitive to diagnose milder forms of HAND (Abidin et al. 2020; Brouillette et al. 2015; Torti et al. 2011). Hence, neuroimaging techniques are also being explored to better understand and aid in early diagnosis of brain abnormalities that occur during HIV (Abidin et al. 2020; Ances and Hammoud 2014; Masters and Ances 2014). The biomarkers

of cognitive impairment found through neuroimaging could be in turn assist in developing more sensitive NP tests.

Over the last two decades resting state functional magnetic resonance imaging (rsfMRI) (Biswal et al. 1995) has become the preeminent neuroimaging technique to examine brain function and its pathology. A seminal study found that regions in brain networks that show co-activation during fMRI task performance are also functionally connected at rest (Laird et al. 2011; Smith et al. 2009). Thus, rsfMRI, which typically involves acquiring just one approximately 10 min blood oxygenation level-dependent (BOLD) fMRI scan while the subjects are at rest, can be used to *quantitatively map the integrity of all brain function networks, as well as interactions between them*, in terms of resting state functional connectivity (FC) between areas in these brain networks (Arnold Anteraper et al. 2019; Buckner et al. 2013; Gopinath et al. 2019). RsfMRI is increasingly being employed to investigate brain function impairment in HIV-positive (HIV+) subjects on cART. RsfMRI studies have revealed impairments in default mode (Abidin et al. 2020; Thomas et al. 2020), executive function and control (Abidin et al. 2020; Chaganti et al. 2017; Thomas et al. 2013), salience (Chaganti et al. 2017; Thomas et al. 2013), visuomotor (Egbert et al. 2018; Wang et al. 2011), cortico-striatal (Ipser et al. 2015; Ortega et al. 2015) and resting state networks. Further, some studies have revealed meaningful correlations between performance in neurocognitive tasks and corresponding brain function networks (Chaganti et al. 2017; Egbert et al. 2018; Wang et al. 2018). However, some other studies have revealed little or no functional connectivity impairments in HAND (Cole et al. 2018; Guha et al. 2016; Janssen et al. 2017).

There are a number of data analysis methods available to probe resting state networks (RSNs). The optimal method for a given rsfMRI study depends on its aims and goals. The preponderance of HIV rsfMRI studies have employed seed based correlation analysis (sbCA) (Chaganti et al. 2017; Guha et al. 2016; Ortega et al. 2015; Thomas et al. 2013; Wang et al. 2018) or its variants (Janssen et al. 2017). This type of analysis works best for symptoms based hypotheses, where there is adequate rationale for choosing a priory seed regions of interest (ROIs). However, symptoms, and impairment on standard neuropsychological (NP) tests may be lacking in some HIV+ individuals, and therefore not sufficient to form appropriate seed ROIs. Hence, hypothesis-independent data-driven rsfMRI analysis methods may be more suitable than sbCA for studying the brain during HIV. In terms of data-driven analysis, some HIV studies have employed independent component analysis (ICA) and found impairments in higher order visual and visuomotor networks (Egbert et al. 2018; Wang et al. 2011). However, since ICA imposes spatial sparsity conditions, it is not very sensitive to impairment in brain areas (e.g., subcortical) where neighboring regions (e.g., dorsal and ventral striatum) can have very disparate functions. A recent study (Abidin et al. 2020) employed graph theory and network analysis with a well-established 160-ROI parcellation of the brain (Dosenbach et al. 2010), finding altered FC in the default mode network, and altered network measures of integration, segregation, and connectedness in some other regions. One problem with 160 ROI Dosenbach atlas (Dosenbach et al. 2010 is that it does not have sufficiently high resolution in sub-cortical areas (e.g., it combines all basal ganglia regions into one ROI).

Here we report on an rsfMRI study we performed as part of a prospective biomarker investigation of HIV+ individuals on cART with minimal neurocognitive symptoms as well as matched HIV-seronegative (HIV−) individuals. Two blood biomarkers (one reflecting neuronal damage and one reflecting inflammation) were also measured to evaluate for potential relationships with rsfMRI. We employed a recently described data driven high-resolution network analysis approach (Anteraper et al. 2020, 2019; Guell et al. 2020) to examine functional connectivity impairments in HIV+ individuals. Briefly, this method examines the rsfMRI functional connectivity (FC) patterns (to the level of individual voxels) of all voxels with multivariate pattern analysis (MVPA) and identifies voxel clusters that best illustrate the differences in FC patterns between HIV+ and matched HIV− individuals. These clusters act as seed ROIs for post hoc sbCA, which would reveal impaired or abnormally high FC in RSNs in HIV+ group, as per our hypotheses. We also examined the relationships between rsfMRI FC and NP assessments, as well as clinical biomarkers.

Methods

Study participants

This neuroimaging study was performed as part of a larger soluble biomarkers study. HIV+ individuals were required to be on a stable cART regimen for at least 3 months. Individuals were excluded from the study for any of the following: (1) history of any neurologic disease known to affect memory (including stroke, malignancy involving the brain, traumatic brain injury, and AIDS-related opportunistic infection of the central nervous system); (2) current ongoing substance use (marijuana use in the last 7 days OR cocaine, heroin, methamphetamine, or other non-marijuana illicit drug use in the last 30 days); (3) heavy alcohol consumption in the last 30 days (defined as > 7 drinks per week for women and > 14 drinks per week for men); (4) serious mental illness including schizophrenia and bipolar disorder; (5) chronic hepatitis C virus (HCV) infection, which was tested for at study entry; or (6) MRI contraindications. Potential participants were screened for uncontrolled depression with the Beck Depression Inventory Fast Screen (BDI-FS) and excluded for a score of ten or higher. Individuals with a history of treated syphilis and a persistently positive rapid

plasma regain (RPR) titer of 1:8 or less were eligible for the study if there was a decrease in RPR of at least fourfold at 6 months after treatment and there were no neurological symptoms at initial syphilis presentation. The fourth-generation Abbott antigen/antibody assay was performed at study entry to confirm seronegativity in the HIV− group. All HIV− participants were confirmed to be HCV seronegative at study entry as well. After screening 16 HIV+ and 12 HIV− subjects participated in the study (see Table 1). The study was approved by the Emory University Institutional Review Board, and written consent was obtained from all participants.

Neuropsychological (NP) battery, laboratory studies, and related statistical analyses: A comprehensive NP testing panel used commonly in studies of cognition and HIV infection (Robertson and Yosief 2014) was included: (1) Trail Making Part A, (2) Trail Making Part B, (3) Hopkins Verbal Learning Test total learning, (4) Hopkins Verbal Learning Test delayed recall, (5) Grooved Pegboard (dominant), (6) Grooved Pegboard (non-dominant), (7) Stroop Color Naming, (8) Stroop Color-Word, (9) Digit Vigilance Test (total time), (10) Digit Vigilance Test (errors), (11) Brief Visual Memory Test total time, (12) Brief Visual Memory Test delayed recall, (13) Finger Tapping test (dominant hand), and (14) Letter Fluency (Controlled Oral Word Association Test). These tests were selected in order to examine at least five domains as recommended in the most recent nosology of HAND criteria (Antinori et al. 2007). Raw scores were adjusted for demographic characteristics using published norms to compute *T* scores (Heaton et al. 2004). Domain *T* scores (average of *T* scores in tests pertaining to individual domain (e.g., memory) or in the event of language just the letter fluency T score) as well as Global *T* score (average of domain T scores) were calculated. Global deficit score (GDS), a validated measure of overall neurocognitive impairment that is resulted based on *T* scores (Carey et al. 2004), was also calculated. Neurofilament light chain (NFL) from plasma

Table 1 Comparisons between HIV positive and negative groups

Variable Median (IQR) or Mean [SD] Number (%)	HIV positive (*n* = 16)	HIV negative (*n* = 12)	*P* value for difference	Effect size
A in years	38 (33–48)	34 (31–45)	0.28	
Male sex	14 (88%)	10 (83%)	1.0	
African-American	15 (94%)	10 (83%)	0.56	
Years of education	13.5 (12–16)	13 (12–14)	0.33	
Co-morbidities	11 (69%)	9 (75%)	1.0	
Cigarette smoker	1 (6.3%)	0 (0%)	1.0	
Hypertension	0 (0%)	0 (0%)	1.0	
Diabetes mellitus	2 (12.5%)	1 (8.3%)	1.0	
Depression				
Laboratory results	258 (82–433)	-	0.29[a]	0.57
CD4+	< 2 (< 2–3.5)	-	0.42[a]	0.4
HIV RNA (log10)	6.49 (4.75–9.56)	4.33 (3.63–9.13)		
NF-L	1.89 (1.23–2.75)	0.88 (0.70–5.64)		
CRP				
Neuropsychological testing				
GDS	0.07 (0.0–0.27)	0.1 (0.0–0.29)	0.88	Effect Size
Global T	51.1 [4.9]	53.0 [4.9]	0.33	0.39
Executive T	50.4 [8.3]	56.0 [10.3]	0.12	0.61
Processing speed T	51.2 [7.1]	55.7 [10.3]	0.18	0.52
Learning T	51.9 [10.0]	52.7 [7.9]	0.83	0.09
Memory T	52.0 [9.2]	51.2 [8.3]	0.81	0.09
Attention T	52.6 [6.7]	47.8 [9.0]	0.12	0.62
Fine Motor T	49.7 [8.3]	53.6 [6.5]	0.2	0.51
Language T	53.3 [7.3]	53.9 [11.1]	0.85	0.07

IQR interquartile range, *SD* standard deviation, *HIV* human immunodeficiency virus infection, *NF-L* neurofilament light chain, *CRP* C-reactive protein, *GDS* global deficit score

[a]Assumes interquartile range is from a normal distribution

was measured using an ultrasensitive assay (Simoa by Quanterix corporation) recently shown by our group to be quantifiable in both HIV+ and HIV− individuals (Anderson et al. 2018). C-reactive protein (performed at Laboratory Corporation of America) was measured as a marker of systemic inflammation. Plasma HIV RNA was measured at the Emory Center for AIDS Research Virology Core using the Abbott Laboratories m2000 Real Time HIV-1 assay system (reverse transcriptase polymerase chain reaction, lowest limit of detection of 40 copies/ml). All of these baseline characteristics data were first assessed for normality with the Shapiro-Wilk test. The Wilcoxon rank sum test was used for comparing continuous variables, unless normality conditions were met, in which case the paired t test was used. Fisher's exact test was used to compare categorical results between groups.

Image acquisition: MR images were acquired on a 3 T Siemens Magnetom Prisma-Fit scanner with a 32-channel receiver array head coil. The participants were instructed to keep their eyes open and look at a fixation cross during the resting-state scans. Blood oxygenation level-dependent (BOLD) contrast rsfMRI scans were acquired using a simultaneous multi-slice (SMS) gradient echo (GE) EPI sequence (Feinberg et al. 2010; Moeller et al. 2010) with imaging parameters: field-of-view (FOV) = 220 mm; repetition time (TR)/echo time (TE) = 1000 ms/26 ms; flip angle (FA) = 60°; 74 × 74 matrix size; 72 axial slices of 2 mm width covering the whole brain; multiband slice-acceleration factor = 6; in-plane generalized autocalibrating partial parallel acquisition (GRAPPA) acceleration factor = 2; 280 scan volumes. Two five-volume spin-echo conventional EPI sequences with the same image resolution, coverage, and TE as the GE EPI sequence described above were also acquired to assist with distortion correction, one with the same direction of phase-encoding (PE) anterior-posterior (AP), and one with reversed PE direction (PA). A whole-brain 3D T1-weighted magnetization prepared rapid gradient echo (MPRAGE) sequence (FOV = 230 mm; TR/TI/TE/FA = 2250 ms/900 ms/3 ms/9°; 0.9 mm×0.9 mm×1 mm resolution; TI = inversion time) provided anatomic detail. Foam padding was provided to minimize subject-motion during the scans.

Data analysis: Preprocessing: Data analysis was performed with AFNI (Cox 1996), FSL (Smith et al. 2004), and CONN (Whitfield-Gabrieli and Nieto-Castanon 2012) toolboxes, employing standard well-established pipelines (Arnold Anteraper et al. 2019; Glasser et al. 2013). The rsfMRI voxel time-series were corrected for geometric distortions, temporally shifted to account for differences in slice acquisition times, 3D volume registered to a base volume to account for global rigid motion. The resultant rsfMRI time-series were co-registered to the T1-weighted high-resolution anatomic scan using the well-established

affine boundary based registration algorithm (Greve and Fischl 2009), and spatially normalized to the MNI152 template with the warp computed from alignment of the high-resolution 3D anatomic to the MNI152 template with a nonlinear registration algorithm. The spatially normalized rsfMRI data were spatially smoothed by with an isotropic Gaussian filter (full-width at half maximum (FWHM) = 6 mm) and band pass filtered (0.008–0.09 Hz). Physiological sources of noise including signals from white matter and CSF were regressed out using the anatomical CompCor method (Behzadi et al. 2007). Spurious correlations in time-series due to head motion were addressed using the Artifact Detection Tool (ART, http://www.nitrc.org/projects/artifact_detect) with outliers defined as rsfMRI volumes showing greater than 0.5 mm frame-to-frame displacement or global mean intensity greater than three standard deviations from the mean intensity of the entire scan. ART outliers along with the six realignment parameters were added as regressors of no interest, so that their effects could be removed from the fMRI time-series. There was no significant difference in head motion, number of outliers, and BOLD variance (after denoising) between groups.

Multivariate pattern analysis: CONN toolbox implementation of whole-brain multi-voxel pattern analysis (MVPA) (Whitfield-Gabrieli and Nieto-Castanon. 2012) was used to detect brain areas with abnormal functional connectivity patterns in HIV+ compared with HIV− subjects. This method is performed in two steps. First, the connectivity matrix (matrix of cross correlations (CC) between all voxel time-series) of each subject was decomposed with principal components analysis (PCA). The first 64 PCs were retained to characterize the salient features of the connectivity matrix. In the second step, jointly across all subjects but separately for each voxel, the 3 strongest components (Thompson et al. 2016) were retained from a PCA decomposition of the between-subjects variability in seed-to-voxel connectivity maps between this voxel and the rest of the brain. Then, an omnibus F test was performed on all 3 MVPA components (which explain the maximum inter-subject variability) simultaneously in a single second-level analysis to identify the voxels that show significant differences in connectivity patterns between the two groups. Clusters surviving a cluster detection threshold (CDT) of $p < 0.05$ and familywise error-corrected threshold of $\alpha < 0.05$ were taken for post hoc analysis.

Post hoc characterization of MVPA-derived clusters: For within and between-group FC post hoc characterization, the three MVPA-derived clusters of interest were used as seed regions of interests (ROIs) for seed-based cross-correlation analysis (sbCCA). Pearson's cross-correlation coefficients between each MVPA cluster-ROI averaged time course, and the time courses of all other voxels in

the brain were computed and then converted to normally distributed *z*-scores using Fisher transformation in order to carry out second-level general linear model analyses. A CDT $p < 0.001$ and false discovery rate (FDR)-corrected threshold of $\alpha < 0.05$ were used. Additionally, a non-parametric permutation analysis (1000 iterations) was used for between-group comparison. This method has been shown to be effective in curbing false positives, thereby adding validity to the cluster size inferences (Eklund et al. 2016), but see also (Gopinath et al. 2018).

Results

Clinical and neuropsychological tests

Sixteen HIV+ adults with chronic infection as well as 12 age/sex/race matched HIV− individuals (see Table 1) were enrolled at the Emory Center for AIDS Research (CFAR) clinical core site in Atlanta, Georgia. There were no significant differences between HIV+ and HIV− groups in terms of demographics or current medical conditions (Table 1). Participants were mostly male and African-American. Among HIV+ participants, the estimated duration of infection was 44 months (interquartile range [IQR] = 25–163 months). While the majority of HIV+ participants had suppressed HIV RNA levels (< 100 copies/ml), 25% had plasma HIV RNA > 1000 copies/ml. With respect to NP test performance, there were no group differences in overall GDS (Table 1) or in the proportion ($p = 0.56$ by Fisher's exact test) of individuals with impairment by GDS (one out of sixteen in the HIV+ group [with GDS = 0.79] and two out of twelve in the HIV-negative group [with GDS = 0.54 and 0.57, respectively]). Also, there were no statistically significant differences between the groups in the domain *T* scores. The effect sizes of the NP test score differences between the two groups as well as those of clinical biomarker differences calculated post hoc ranged from small to moderate (Cohen 2013; Faul et al. 2009).

Table 2 Brain regions overlapping each MVPA-derived cluster of brain voxels exhibiting significant (CDT $p < 0.05$; FDR $\alpha < 0.05$) differences in FC patterns between HIV+ and HIV− groups

	Brain regions	Cluster-peak coordinates (MNI)	Voxels per cluster
(1)	Primary visual cortex	18 − 70 06	331
(2)	Cerebellar Crus I/II	− 36 − 76 − 50	323
(3)	Inferior frontal gyrus	− 54 36 06	274

Resting state fMRI: MVPA results

MVPA analysis revealed three clusters which exhibited significant (CDT $p < 0.05$; FDR $\alpha < 0.05$) differences in FC patterns between HIV+ and HIV− groups. These clusters were located (Fig. 1; Table 2) in right primary visual cortex (V1), left cerebellum Crus I/II, and left inferior frontal gyrus (IFG).

Post hoc characterization of MVPA clusters

The right primary visual cortex (V1) MVPA cluster exhibited (Fig. 1) significant FC with visual processing brain areas (primary and extrastriate visual cortices, as well as occipitotemporal cortex) and locations in the dorsal and ventral visual streams, in both HIV+ and HIV− groups. However, HIV+ subjects exhibited significantly *reduced FC* compared with HIV− subjects (Figs. 2 and 3; Table 3) between V1 cluster and bilateral anterior supramarginal gyrus (SMG). HIV+ group also exhibited *reduced* FC between left cerebellum crus I/II cluster and right hemisphere areas, frontal/premotor eye fields, and lateral frontal pole, as well as left lateral occipital complex. Finally, HIV+ group also exhibited *reduced* FC between the left IFG cluster and intraparietal sulcus, its adjacent inferior parietal lobule, and cerebellum crus II in the left hemisphere, and right angular gyrus. On the other hand, HIV+ group exhibited *increased* FC between left IFG and

Fig. 1 MVPA between-group results (CDT $p < 0.05$, and FDR-corrected $\alpha < 0.05$) revealing abnormal connectivity in the three clusters: one each in primary visual cortex, cerebellum crus I/II, and inferior frontal gyrus. See Table 2 for description of the 3 clusters
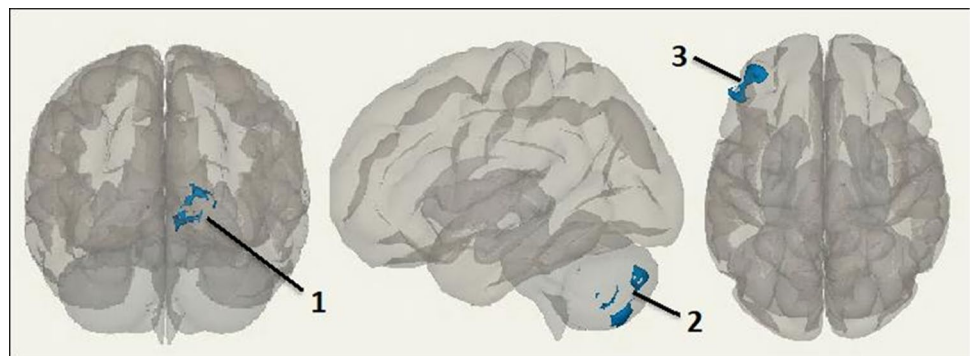
Fig. 2 Post hoc characterization of MVPA clusters: Results from post hoc seed-to-voxel group FC comparison using MVPA clusters (shown in Fig. 1) as seed ROIs. Brain FC results for HIV + group main effect and HIV-group main effect for the three MVPA clusters are shown in cortical maps in panels **a**, **b**, and **c** respectively. Brain regions indicated by numbers in (A), (B), and (C) correspond to clusters exhibiting significant (CDT $p < 0.001$; FDR-corrected $\alpha < 0.05$) differences in FC between HIV+ HIV−, as described in Table 3. The cluster in the cerebellum (cluster #9) is presented on a flat map
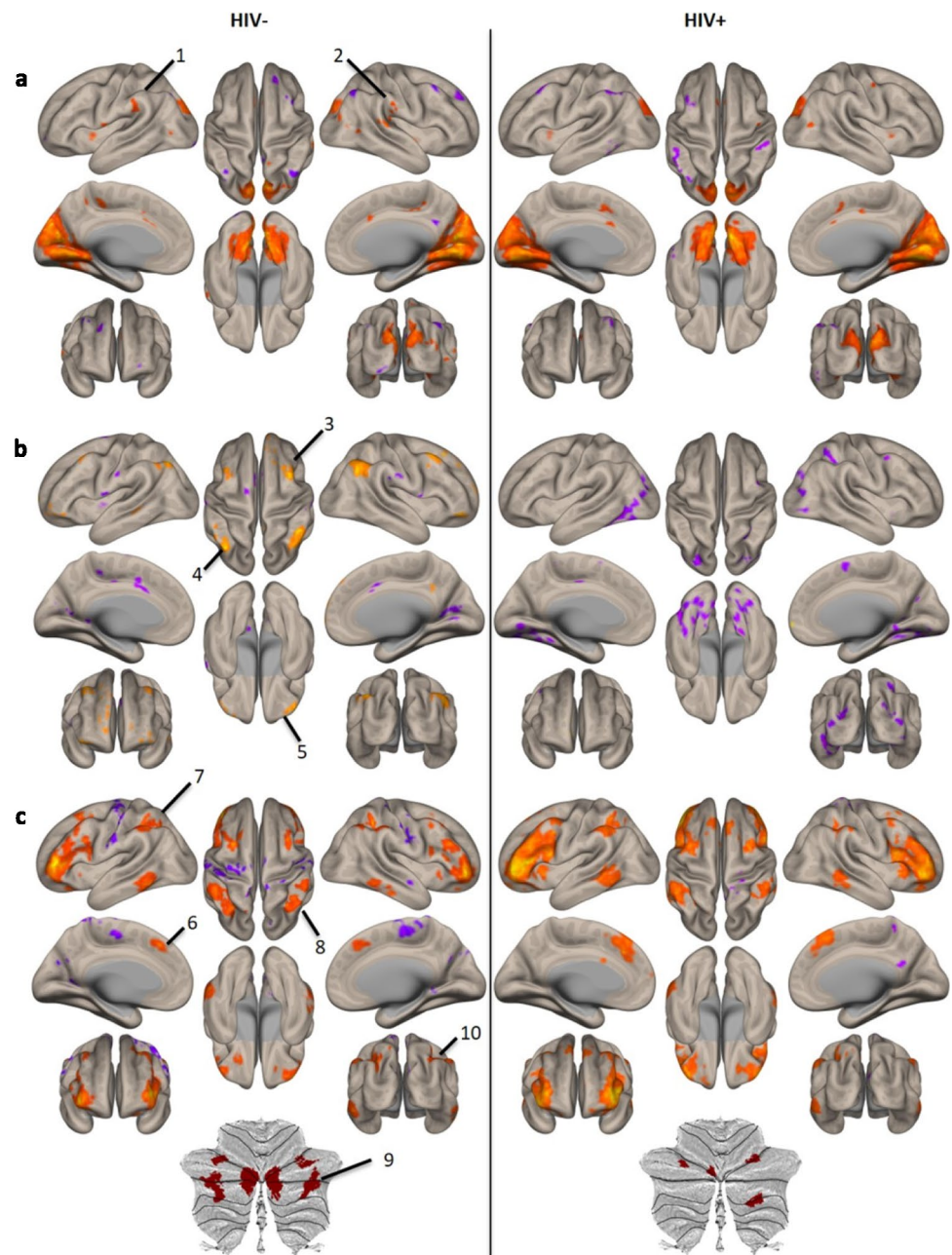
right pre-supplementary motor area (pre-SMA). The effect sizes of the FC differences between groups were very large (Table 3). There were no significant relationships between the FCs and any of the neurocognitive test domain *T* scores.

Discussion

HIV+ subjects exhibit fMRI impairments

Chronic HIV infection continues to be associated with multiple CNS sequelae, including HAND. However, NP performance has been shown to be insensitive to detecting some CNS sequelae. For example, HIV CNS virologic escape is often not associated with NP impairment, even with comprehensive testing (Perez-Valero et al. 2019). In this study we did not find significant differences between HIV+ and HIV− groups in their performance in NP tests (Table 1). Effect size calculations revealed that executive function and attention *T* scores would have been significant if the sample size was increased to around 70 for each group (see Supplementary Table 1). Similarly, fine motor would have been significant if the sample size was increased to around 100 for each group, which is within the realm of

Fig. 3 HIV+ and HIV− group box plots of resting state functional connectivity (RsFC) strengths (peak *z*-scores) for each of the clusters enumerated in Table 3
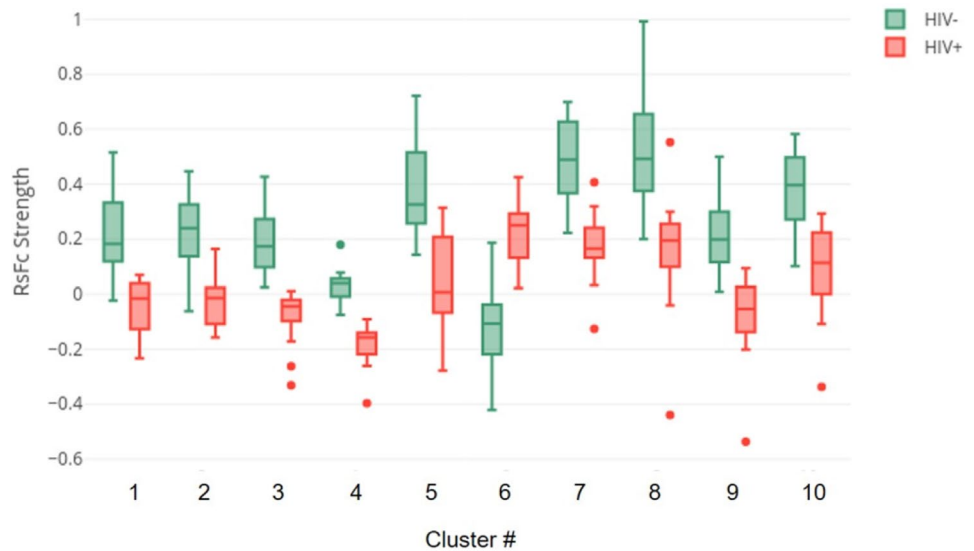
some large sample size HIV studies (Heaton et al. 2010). However, learning, memory, and language NP test effect sizes were too small to be detected with reasonable sample sizes. Both groups also did not reveal significant differences in assays of neurofilament-light chain (NF-L) and c-reactive protein (CRP), which are markers of axonal damage and neuroinflammation respectively (Table 1). On the other hand, resting state fMRI revealed impaired FC in a number of brain function networks. HIV+ group exhibited significantly decreased FC between primary visual cortex and the somatosensory association areas in bilateral anterior supramarginal, indicating decreased capacity for multisensory integration in HIV+ patients. This is consistent with impairments in visuomotor and visuospatial functions seen in some HIV studies (Agarwal et al. 2020; Egbert et al. 2018; Gawron et al. 2019; Wang

et al. 2011). To our knowledge, this is the first fMRI study which has revealed impaired FC in multisensory processing networks in HIV+ subjects, though some other studies have shown impairment in higher order visual processing (lateral occipital complex) (Wang et al. 2011) and visuomotor networks (Egbert et al. 2018). HIV+ subjects also exhibited reduced FC between left cerebellum crus I/II and right hemisphere frontal areas that subserve attention and cognition (Baumann et al. 2015; Stoodley et al. 2012). This is consistent with attention and executive function impairments seen in HIV studies (Gawron et al. 2019; Ortega et al. 2015), including those employing rsfMRI to examine brain function (Abidin et al. 2020; Chaganti et al. 2017; Ipser et al. 2015; Thomas et al. 2013). Finally, HIV+ subjects exhibited *reduced* FC between left IFG and parietal language areas, e.g., those seen in semantic

Table 3 Post hoc characterization of MPVA clusters: Results from second-level FC analysis using the three MVPA-derived seed ROIs for HIV+ versus HIV− contrast. A CDT $p < 0.001$ (two-sided), and FDR-corrected $\alpha < 0.05$ (parametric statistics) was used for post hoc characterization. Significant clusters in the 3 FC analyses are enumerated, along with mean T across the cluster, along with its effect size. The cluster numbers are marked on cortical maps by corresponding arrows in Fig. 2. The distribution of resting state FCs across the two groups for each cluster is shown in Fig. 3

Cluster numbers	Region	Peak cluster coordinates (MNI)	Voxels per cluster	T_{mean}	Effect size
	Regions exhibiting HIV+ vs HIV− differences in FC to primary visual cortex cluster				
1	Left anterior supramarginal gyrus	− 58 − 32 30	113	− 5.68	2.2
2	Right anterior supramarginal gyrus	60 − 26 32	48	− 5.25	2.0
	Regions exhibiting HIV+ vs HIV− differences in FC to left Cerebellum Crus I/II Cluster				
3	Right frontal/premotor eye fields	42 06 48	99	− 6.42	2.4
4	Left lateral occipital complex	− 42 − 56 − 20	62	− 8.00	3.1
5	Right lateral frontal pole	22 62 22	49	− 4.86	1.9
	Regions exhibiting HIV+ vs HIV− differences in FC to left inferior frontal gyrus cluster				
6	Right pre-supplementary motor area	8 28 58	78	+ 6.31	2.4
7	Left intra-parietal sulcus	− 42 − 50 50	55	− 5.69	2.2
8	Left inferior parietal lobule	− 32 − 70 50	54	− 4.61	1.7
9	Left cerebellum crus II	− 10 − 84 − 32	45	− 5.34	2.0
10	Right angular gyrus	38 − 60 50	35	− 4.96	1.9

word generation fMRI studies (Crosson et al. 2003, 1999). On the other hand, HIV+ subjects exhibited *increased* FC between left IFG and right pre-SMA. Since neural activity in right hemisphere frontal structures interfere with language production (Crosson et al. 2005), this abnormally increased FC could induce deficits in language function in HIV+ subjects (Crosson et al. 2005). These results are consistent with language impairments (Binder 2017; Crosson et al. 2005) seen in some HIV studies (Agarwal et al. 2020; Mapstone et al. 2013). To our knowledge, this is the first rsfMRI study that has revealed impaired FC in language function networks in HIV+ subjects.

The effect sizes of all these rsfMRI FC results were very large (Table 3), in contrast with the small effect sizes seen in NP tests (Table 1), which rendered them non-significant. Thus, rsfMRI may be able to detect cognitive impairment with much greater sensitivity than NPs. In this regard, our results are consistent with another fMRI study which revealed impairments in face processing network in HIV+ subjects in the absence of behavioral deficits (Liu et al. 2015). These preliminary results indicate the promise of finding predictive biomarkers for CNS impairments in HIV, based on rsfMRI FC techniques.

Limitations

One of the limitations of our study was that the sample size of HIV+ and HIV− subjects was small, and therefore, our power to find statistically significant differences was likely limited, especially with regard to NP tests. Further, four HIV+ subjects were not virally suppressed (plasma RNA > 1000 cp/ml). However, removing these four subjects from analysis did not qualitatively change the outcomes (see Supplementary Results). There were no significant relationships between the FCs (in different networks exhibiting differences between HIV+ and HIV− groups) and any of the neurocognitive test domain *T* scores. This could be related to the lack of significance seen in NP testing differences between the groups. Additionally, only one test of language function was performed, and typically, two tests are considered necessary for full evaluation. This hindered the appropriate evaluation of relationship between impaired FCs in the language function networks and neurocognitive assessment of the language domain in HIV+ subjects. While none of the NP tests performed evoked significance differences at $p < 0.05$, power analysis revealed that the tests for executive function and attention, as well as to a lesser extent fine-motor and processing speed, could have been significant (at $p < 0.05$) with larger sample sizes (see Supplementary Table 1) seen in some HIV studies. Further, only blood biomarkers of neurofilament light and c-reactive proteins could be obtained. CSF biomarkers are likely to be more sensitive to CNS abnormalities. Finally, it must be noted that more than 80% of our HIV+ and HIV− cohorts were male. While the majority of HIV+ individuals in the USA are male (approximately 80%) (CDC), a significant minority are women. Given that sex appears to play a role in fMRI findings, our results may not be generalizable to women. More research is needed on fMRI in HIV-infected women. Also, 94% in HIV+ and 83% in HIV− group were African American. While the majority of new HIV cases in the southeastern USA are in African Americans (CDC), ideally, our study would have had more racial/ethnic diversity.

Conclusion

In this study, we examined 16 HIV+ subjects and 12 age, sex, and race matched seronegative subjects with NP testing, blood assays, in addition to resting state fMRI. While NP testing and biomarkers for neuroinflammation and axonal damage did not reveal significant differences in HIV+ subjects, advanced network analysis of rsfMRI data revealed significant impairment in language, attention, executive function, and multisensory perception domains. The results indicate that rsfMRI employing advanced data analysis techniques can be a very sensitive biomarkers for CNS damage in HIV+ individuals.

References

Abidin AZ, AM DS, Schifitto G, Wismuller A (2020) Detecting cognitive impairment in HIV-infected individuals using mutual connectivity analysis of resting state functional MRI. J Neurovirol 26:188–200

Agarwal R, Aujla RS, Gupta A, Kumar M (2020) Determining the neurocognitive status and the functional ability of patients to screen for HIV-Associated Neurocognitive Disorder (HAND). Dement Neurocogn Disord 19:19–27

Ances BM, Hammoud DA (2014) Neuroimaging of HIV-associated neurocognitive disorders (HAND). Curr Opin HIV AIDS 9:545–551

Anderson AM, Easley KA, Kasher N, Franklin D, Heaton RK, Zetterberg H, Blennow K, Gisslen M, Letendre SL (2018) Neurofilament light chain in blood is negatively associated with neuropsychological performance in HIV-infected adults and declines with initiation of antiretroviral therapy. J Neurovirol 24:695–701

Anderson AM, Schein TN, Kalapila A, Lai L, Waldrop-Valverde D, Moore RC, Franklin D, Letendre SL, Barnum SR (2017). Soluble membrane attack complex in the blood and cerebrospinal fluid of HIV-infected individuals, relationship to HIV RNA, and comparison with HIV negatives. J Neuroimmunol.

Anteraper SA, Collin G, Guell X, Scheinert T, Molokotos E, Henriksen MT, Mesholam-Gately R, Thermenos HW, Seidman LJ, Keshavan MS, Gabrieli JDE, Whitfield-Gabrieli S (2020) Altered resting-state functional connectivity in young children at familial high risk for psychotic illness: a preliminary study. Schizophr Res 216:496–503

Anteraper SA, Guell X, Taylor HP, D'Mello A, Whitfield-Gabrieli S, Joshi G (2019) Intrinsic functional connectivity of dentate nuclei in autism spectrum disorder. Brain Connect 9:692–702

Antinori A, Arendt G, Becker JT, Brew BJ, Byrd DA, Cherner M, Clifford DB, Cinque P, Epstein LG, Goodkin K, Gisslen M, Grant I, Heaton RK, Joseph J, Marder K, Marra CM, McArthur JC, Nunn M, Price RW, Pulliam L, Robertson KR, Sacktor N, Valcour V, Wojna VE (2007) Updated research nosology for HIV-associated neurocognitive disorders. Neurology 69:1789–1799

Arnold Anteraper S, Guell X, D'Mello A, Joshi N, Whitfield-Gabrieli S, Joshi G (2019) Disrupted cerebrocerebellar intrinsic functional connectivity in young adults with high-functioning autism spectrum disorder: a data-driven, whole-brain, high-temporal resolution functional magnetic resonance imaging study. Brain Connect 9:48–59

Baumann O, Borra RJ, Bower JM, Cullen KE, Habas C, Ivry RB, Leggio M, Mattingley JB, Molinari M, Moulton EA, Paulin MG, Pavlova MA, Schmahmann JD, Sokolov AA (2015) Consensus paper: the role of the cerebellum in perceptual processes. Cerebellum 14:197–220

Behzadi Y, Restom K, Liau J, Liu TT (2007) A component based noise correction method (CompCor) for BOLD and perfusion based fMRI. Neuroimage 37:90–101

Binder JR (2017) Current controversies on Wernicke's Area and its role in language. Curr Neurol Neurosci Rep 17:58

Biswal B, Yetkin FZ, Haughton VM, Hyde JS (1995) Functional connectivity in the motor cortex of resting human brain using echo-planar MRI. Magn Reson Med 34:537–541

Brouillette MJ, Mayo N, Fellows LK, Lebedeva E, Higgins J, Overton ET, Ances BM, Koski L (2015) A better screening tool for HIV-associated neurocognitive disorders: is it what clinicians need? AIDS 29:895–902

Buckner RL, Krienen FM, Yeo BT (2013) Opportunities and limitations of intrinsic functional connectivity MRI. Nat Neurosci 16:832–837

Carey CL, Woods SP, Gonzalez R, Conover E, Marcotte TD, Grant I, Heaton RK, Group H (2004) Predictive validity of global deficit scores in detecting neuropsychological impairment in HIV infection. J Clin Exp Neuropsychol 26:307–319

Chaganti JR, Heinecke A, Gates TM, Moffat KJ, Brew BJ (2017) Functional connectivity in virally suppressed patients with HIV-associated neurocognitive disorder: a resting-state analysis. AJNR Am J Neuroradiol 38:1623–1629

Cohen J (2013). Statistical power analysis for the behavioral sciences. Academic press.

Cole JH, Caan MWA, Underwood J, De Francesco D, van Zoest RA, Wit F, Mutsaerts H, Leech R, Geurtsen GJ, Portegies P, Majoie C, Schim van der Loeff MF, Sabin CA, Reiss P, Winston A, Sharp DJ, Comorbidity in Relations to AC (2018) No Evidence for Accelerated Aging-Related Brain Pathology in Treated Human Immunodeficiency Virus: Longitudinal Neuroimaging Results From the Comorbidity in Relation to AIDS (COBRA) Project. Clin Infect Dis 66:1899

Cox RW (1996) AFNI: software for analysis and visualization of functional magnetic resonance neuroimages. Comput Biomed Res 29:162–173

Crosson B, Benefield H, Cato MA, Sadek JR, Moore AB, Wierenga CE, Gopinath K, Soltysik D, Bauer RM, Auerbach EJ, Gokcay D, Leonard CM, Briggs RW (2003) Left and right basal ganglia and frontal activity during language generation: contributions to lexical, semantic, and phonological processes. J Int Neuropsychol Soc 9:1061–1077

Crosson B, Moore AB, Gopinath K, White KD, Wierenga CE, Gaiefsky ME, Fabrizio KS, Peck KK, Soltysik D, Milsted C, Briggs RW, Conway TW, Gonzalez Rothi LJ (2005) Role of the right and left hemispheres in recovery of function during treatment of intention in aphasia. J Cogn Neurosci 17:392–406

Crosson B, Radonovich K, Sadek JR, Gokcay D, Bauer RM, Fischler IS, Cato MA, Maron L, Auerbach EJ, Browd SR, Briggs RW (1999) Left-hemisphere processing of emotional connotation during word generation. NeuroReport 10:2449–2455

Dosenbach NU, Nardos B, Cohen AL, Fair DA, Power JD, Church JA, Nelson SM, Wig GS, Vogel AC, Lessov-Schlaggar CN, Barnes KA, Dubis JW, Feczko E, Coalson RS, Pruett JR Jr, Barch DM, Petersen SE, Schlaggar BL (2010) Prediction of individual brain maturity using fMRI. Science 329:1358–1361

Egbert AR, Biswal B, Karunakaran K, Gohel S, Pluta A, Wolak T, Szymanska B, Firlag-Burkacka E, Sobanska M, Gawron N, Bienkowski P, Sienkiewicz-Jarosz H, Scinska-Bienkowska A, Bornstein R, Rao S, Lojek E (2018) Age and HIV effects on resting state of the brain in relationship to neurocognitive functioning. Behav Brain Res 344:20–27

Eklund A, Nichols TE, Knutsson H (2016) Cluster failure: Why fMRI inferences for spatial extent have inflated false-positive rates. Proc Natl Acad Sci U S A 113:7900–7905

Faul F, Erdfelder E, Buchner A, Lang AG (2009) Statistical power analyses using G*Power 3.1: tests for correlation and regression analyses. Behav Res Methods 41:1149–1160

Feinberg DA, Moeller S, Smith SM, Auerbach E, Ramanna S, Glasser MF, Miller KL, Ugurbil K, Yacoub E (2010) Multiplexed echo planar imaging for sub-second whole brain FMRI and fast diffusion imaging. PLoS One 5:e15710

Gawron N, Choinski M, Szymanska-Kotwica B, Pluta A, Sobanska M, Egbert AR, Desowska A, Wolak T, Horban A, Firlag-Burkacka E, Bienkowski P, Sienkiewicz-Jarosz H, Scinska-Bienkowska A, Biswal B, Rao SM, Bornstein R, Lojek E (2019) Effects of age, HIV, and HIV-associated clinical factors on neuropsychological functioning and brain regional volume in HIV+ patients on effective treatment. J Neurovirol 25:9–21

Glasser MF, Sotiropoulos SN, Wilson JA, Coalson TS, Fischl B, Andersson JL, Xu J, Jbabdi S, Webster M, Polimeni JR, Van Essen DC, Jenkinson M (2013) The minimal preprocessing pipelines for the Human Connectome Project. Neuroimage 80:105–124

Gopinath K, Krishnamurthy V, Sathian K (2018) Accounting for non-Gaussian sources of spatial correlation in parametric functional magnetic resonance imaging paradigms I: revisiting cluster-based inferences. Brain Connect 8:1–9

Gopinath KS, Sakoglu U, Crosson BA, Haley RW (2019) Exploring brain mechanisms underlying Gulf War Illness with group ICA based analysis of fMRI resting state networks. Neurosci Lett 701:136–141

Grant I, Franklin DR Jr, Deutsch R, Woods SP, Vaida F, Ellis RJ, Letendre SL, Marcotte TD, Atkinson JH, Collier AC, Marra CM, Clifford DB, Gelman DB, McArthur JC, Morgello S, Simpson DM, McCutchan JA, Abramson I, Gamst A, Fennema-Notestine C, Smith DM, Heaton RK, Group C (2014) Asymptomatic HIV-associated neurocognitive impairment increases risk for symptomatic decline. Neurology 82:2055–2062

Greve DN, Fischl B (2009) Accurate and robust brain image alignment using boundary-based registration. Neuroimage 48:63–72

Guell X, D'Mello AM, Hubbard NA, Romeo RR, Gabrieli JDE, Whitfield-Gabrieli S, Schmahmann JD, Anteraper SA (2020) Functional territories of human dentate nucleus. Cereb Cortex 30:2401–2417

Guha A, Wang L, Tanenbaum A, Esmaeili-Firidouni P, Wendelken LA, Busovaca E, Clifford K, Desai A, Ances BM, Valcour V (2016) Intrinsic network connectivity abnormalities in HIV-infected individuals over age 60. J Neurovirol 22:80–87

Harezlak J, Buchthal S, Taylor M, Schifitto G, Zhong J, Daar E, Alger J, Singer E, Campbell T, Yiannoutsos C, Cohen R, Navia B, Consortium HIVN (2011) Persistence of HIV-associated cognitive impairment, inflammation, and neuronal injury in era of highly active antiretroviral treatment. AIDS 25:625–633

Heaton RK, Clifford DB, Franklin DR Jr, Woods SP, Ake C, Vaida F, Ellis RJ, Letendre SL, Marcotte TD, Atkinson JH, Rivera-Mindt M, Vigil OR, Taylor MJ, Collier AC, Marra CM, Gelman BB, McArthur JC, Morgello S, Simpson DM, McCutchan JA, Abramson I, Gamst A, Fennema-Notestine C, Jernigan TL, Wong J, Grant I, Group C (2010) HIV-associated neurocognitive disorders persist in the era of potent antiretroviral therapy: CHARTER Study. Neurology 75:2087–2096

Heaton RK, Miller SW, Taylor MJ, Grant I (2004). Revised Comprehensive norms for an expanded Halstead- Reitan Battery: Demographically adjusted neuropsycho- logical norms for African American and Caucasian adults scoring program (2004).

Ipser JC, Brown GG, Bischoff-Grethe A, Connolly CG, Ellis RJ, Heaton RK, Grant I, Translational Methamphetamine ARCG (2015) HIV infection is associated with attenuated frontostriatal intrinsic connectivity: a preliminary study. J Int Neuropsychol Soc 21:203–213

Janssen MAM, Hinne M, Janssen RJ, van Gerven MA, Steens SC, Goraj B, Koopmans PP, Kessels RPC (2017) Resting-state subcortical functional connectivity in HIV-infected patients on long-term cART. Brain Imaging Behav 11:1555–1560

Laird AR, Fox PM, Eickhoff SB, Turner JA, Ray KL, McKay DR, Glahn DC, Beckmann CF, Smith SM, Fox PT (2011) Behavioral interpretations of intrinsic connectivity networks. J Cogn Neurosci 23:4022–4037

Lamers SL, Rose R, Maidji E, Agsalda-Garcia M, Nolan DJ, Fogel GB, Salemi M, Garcia DL, Bracci P, Yong W, Commins D, Said J, Khanlou N, Hinkin CH, Sueiras MV, Mathisen G, Donovan S, Shiramizu B, Stoddart CA, McGrath MS, Singer EJ (2016) HIV DNA is frequently present within pathologic tissues evaluated at autopsy from combined antiretroviral therapy-treated patients with undetectable viral loads. J Virol 90:8968–8983

Liu C, Wang C, Leclair M, Young M, Jiang X (2015) Reduced neural specificity in middle-aged HIV+ women in the absence of behavioral deficits. Neuroimage Clin 8:667–675

Mapstone M, Hilton TN, Yang H, Guido JJ, Luque AE, Hall WJ, Dewhurst S, Shah K (2013) Poor aerobic fitness may contribute to cognitive decline in HIV-infected older adults. Aging Dis 4:311–319

Masters MC, Ances BM (2014) Role of neuroimaging in HIV-associated neurocognitive disorders. Semin Neurol 34:89–102

Moeller S, Yacoub E, Olman CA, Auerbach E, Strupp J, Harel N, Ugurbil K (2010) Multiband multislice GE-EPI at 7 tesla, with 16-fold acceleration using partial parallel imaging with application to high spatial and temporal whole-brain fMRI. Magn Reson Med 63:1144–1153

Ortega M, Baker LM, Vaida F, Paul R, Basco B, Ances BM (2015) Physical activity affects brain integrity in HIV+ individuals. J Int Neuropsychol Soc 21:880–889

Perez-Valero I, Ellis R, Heaton R, Deutsch R, Franklin D, Clifford DB, Collier A, Gelman B, Marra C, McCutchan JA, Navis A, Sacktor N, Simpson D, Grant I, Letendre S (2019) Cerebrospinal fluid viral escape in aviremic HIV-infected patients receiving antiretroviral therapy: prevalence, risk factors and neurocognitive effects. AIDS 33:475–481

Robertson K, Yosief S (2014) Neurocognitive assessment in the diagnosis of HIV-associated neurocognitive disorders. Semin Neurol 34:21–26

Smith SM, Fox PT, Miller KL, Glahn DC, Fox PM, Mackay CE, Filippini N, Watkins KE, Toro R, Laird AR, Beckmann CF (2009) Correspondence of the brain's functional architecture during activation and rest. Proc Natl Acad Sci U S A 106:13040–13045

Smith SM, Jenkinson M, Woolrich MW, Beckmann CF, Behrens TE, Johansen-Berg H, Bannister PR, De Luca M, Drobnjak I, Flitney DE, Niazy RK, Saunders J, Vickers J, Zhang Y, De Stefano N, Brady JM, Matthews PM (2004) Advances in functional and structural MR image analysis and implementation as FSL. Neuroimage 23(Suppl 1):S208–S219

Stoodley CJ, Valera EM, Schmahmann JD (2012) Functional topography of the cerebellum for motor and cognitive tasks: an fMRI study. Neuroimage 59:1560–1570

Thomas JB, Brier MR, Snyder AZ, Vaida FF, Ances BM (2013) Pathways to neurodegeneration: effects of HIV and aging on resting-state functional connectivity. Neurology 80:1186–1193

Thomas RM, Gallo S, Cerliani L, Zhutovsky P, El-Gazzar A, van Wingen G (2020) Classifying autism spectrum disorder using the temporal statistics of resting-state functional mri data with 3D convolutional neural networks. Front Psych 11:440

Thompson WH, Thelin EP, Lilja A, Bellander BM, Fransson P (2016) Functional resting-state fMRI connectivity correlates with serum levels of the S100B protein in the acute phase of traumatic brain injury. Neuroimage Clin 12:1004–1012

Torti C, Foca E, Cesana BM, Lescure FX (2011) Asymptomatic neurocognitive disorders in patients infected by HIV: fact or fiction? BMC Med 9:138

Tozzi V, Balestra P, Galgani S, Murri R, Bellagamba R, Narciso P, Antinori A, Giulianelli M, Tosi G, Costa M, Sampaolesi A, Fantoni M, Noto P, Ippolito G, Wu AW (2003) Neurocognitive performance and quality of life in patients with HIV infection. AIDS Res Hum Retroviruses 19:643–652

Vivithanaporn P, Heo G, Gamble J, Krentz HB, Hoke A, Gill MJ, Power C (2010) Neurologic disease burden in treated HIV/AIDS predicts survival: a population-based study. Neurology 75:1150–1158

Wang H, Li R, Zhou Y, Wang Y, Cui J, Nguchu BA, Qiu B, Wang X, Li H (2018) Altered cerebro-cerebellum resting-state functional connectivity in HIV-infected male patients. J Neurovirol 24:587–596

Wang X, Foryt P, Ochs R, Chung JH, Wu Y, Parrish T, Ragin AB (2011) Abnormalities in resting-state functional connectivity in early human immunodeficiency virus infection. Brain Connect 1:207–217

Whitfield-Gabrieli S, Nieto-Castanon A (2012) Conn: a functional connectivity toolbox for correlated and anticorrelated brain networks. Brain Connect 2:125–141

https://www.cdc.gov/hiv/statistics/overview/index.html, accessed December 2020